

EURO-COST

**STATISTICAL DISTRIBUTION OF INCIDENT WAVES TO MOBILE ANTENNA
IN MICROCELLULAR ENVIRONMENT AT 2.15 GHz**

Abstract: This paper presents measured statistical distributions of incident waves to a mobile antenna in urban microcellular and indoor environments at 2.15 GHz. The power spectra of azimuth angle, elevation angle, and Doppler frequency are presented for horizontally and vertically polarized waves separately. The measurement campaign has been performed using a spherical dual-polarized antenna array and a wideband radio channel sounder with 30 MHz chip frequency.

Kimmo Kalliola^{1,2} and Heikki Laitinen³

¹ IRC/Radio Laboratory, Helsinki University of Technology, P.O.Box 3000, FIN-02015 HUT, Finland

² Nokia Research Center, P.O.Box 407, FIN-00045 Nokia Group, Finland

³ VTT Information Technology, Telecommunications, P.O.Box 1202, FIN-02044 VTT, Finland

1. Introduction

The mobile radio channel is characterized by the propagation environment. Multipath propagation causes spreading of both azimuth and elevation angles of the incident waves. In multipath environments, the performance of a mobile handset antenna does not depend only on the gain of the antenna, but on the mutual relation between the radiation pattern and the radio environment.

In this paper we present measured statistical distributions of incident waves to a mobile antenna in microcellular environment at 2.15 GHz. The power spectra of azimuth angle, elevation angle, and Doppler frequency are presented. The measurement campaign was performed using a spherical 32-element dual-polarized antenna array and a wideband radio channel sounder with 30 MHz chip frequency. The azimuth and elevation angles of both the vertically polarized (VP) and horizontally polarized (HP) components of the incident waves were measured with 33 ns delay resolution. Both indoor and outdoor mobile routes were measured with a single base station site.

2. Background

In multipath environments, the mean effective gain (MEG) of an antenna defines the power received by the antenna. MEG depends on the radiation pattern of the antenna and the statistical distribution of the incident radio waves in the environment [1]. Specifically, it depends on both the statistical propagation properties of both the VP and HP components of the incident waves. The MEG of an antenna is written as

$$MEG = \int_0^{2\pi} \int_0^{\pi} \left[\frac{P_V}{P_V + P_H} G_\theta(\theta, \phi) P_\theta(\theta, \phi) + \frac{P_H}{P_V + P_H} G_\phi(\theta, \phi) P_\phi(\theta, \phi) \right] \sin \theta d\theta d\phi \quad (1)$$

where $G_\theta(\theta, \phi)$ and $G_\phi(\theta, \phi)$ are the θ and ϕ polarized components of the antenna power gain pattern, respectively. Terms $P_\theta(\theta, \phi)$ and $P_\phi(\theta, \phi)$ are the θ and ϕ polarized components of the angular density functions of the incoming plane waves, respectively. P_V and P_H are the mean incident powers of the VP and HP incident waves received while the antenna moves in the environment, averaged over a random route [1].

When a mobile antenna moves randomly in an environment described by reflections, scattering, and diffraction, the angular density functions of both VP and HP waves can be considered uniform in azimuth [1]. The dispersion of angular density functions in elevation depends strongly on the environment. In [1], Taga proposes a Gaussian distribution of incident waves in elevation for both the VP and HP waves separately. Previously, Aulin [2] has proposed a discontinuous rectangular/sinusoidal angular density function in elevation, which Parsons [3] has modified and proposes a smoother sinusoidal function that also leads to a smoother Doppler spectrum. In addition, Vaughan [4] has proposed a uniform angular density function between 0° and 30° . Taga's model is the only one that takes into account the polarization dependence of the angular density function.

3. Measurement system

The measurement system used in this measurement campaign has been described in [5]. The system is based on a spherical array of 32 dual-polarized antenna elements connected to a wideband radio channel sounder via a fast RF switch. It measures the complex impulse response (IR) of the radio channel in each array element for both θ and ϕ polarized waves, separately. The radius of the array

is 170 mm (1.22λ at the measurement frequency of 2154 MHz). The azimuth and elevation angles of the incident waves can be computed from the relative phases of the elements.

The element of the array is a stacked dual-polarized microstrip patch antenna with separate probe feeds for θ and ϕ polarizations. The 6-dB beamwidth of the element is 90° in the E-plane and 100° in the H-plane. The polarization discrimination is better than 18 dB within 6-dB beamwidth. The measured gain of the element is 7.8 dBi. A photograph of the spherical array used in the measurements is shown in Figure 1.



Figure 1. Spherical array of 32 dual-polarized microstrip patch elements.

4. Description of measurements

The measurements were performed in urban and indoor mobile routes using one base station site. The measurement environment was a downtown shopping area in Helsinki. The surroundings of the outdoor mobile route consists of a dense building structure with narrow alleys and underpasses. The indoor route consists of open lobby and a narrow corridor. The transmitter antenna at the fixed (base) station was a modified GSM1800 base station antenna. The 6-dB beamwidth of the transmitter antenna is 120° in horizontal and 40° in vertical plane. The gain of the antenna is +17 dBi and the transmitted polarization is vertical. The 32-element dual-polarized spherical array was used as the mobile antenna. The array was placed on a motorized trolley, at height of 1.65 m from ground level. The speed of the trolley was constant 0.35 m/s, and 5 impulse responses per wavelength were measured. The used code length was 63 chips resulting in delay window of 2.1 μ s at the used 30 MHz chip frequency. The measurements were performed at night time.

The base station antenna was located on top of a 4m-high mast at the edge of an open car park at the 3rd floor of an office building, approximately 8 m above ground. The BS location is marked in Figure 2 that presents a floor plan of the measurement site. The view from the base station location towards the direction of the mobile routes is shown in Figure 3, and the view from point ① (see Fig. 2) towards BS in Figure 4. Also the mobile routes are marked in Figure 2. Table 1 presents the lengths of the mobile routes and the number of impulse responses recorded along each route from each array element and polarization.

The NLOS indoor measurement route (Route A) begins in an open lobby ③ with the separating walls made of glass, and continues in a corridor ④ with concrete walls close to the mobile antenna. The height of the ceiling is some 4 m in the lobby and 2.5 m in the corridor. The floor level at the door leading into the lobby is 1 m higher than the floor level of the mobile route. The transmitted waves travel mainly through the glass door to the lobby, and further into the corridor. At some point, waves arriving to the mobile from the opposite direction begin to dominate. They are assumed to have traveled through the outdoor passage, and reflected from the building across the street. The outdoor mobile route (Route B) begins in an open square just in front of the BS. The LOS disappears when the mobile goes behind a corner and passes under a bridge ⑤, see Fig. 3 a.

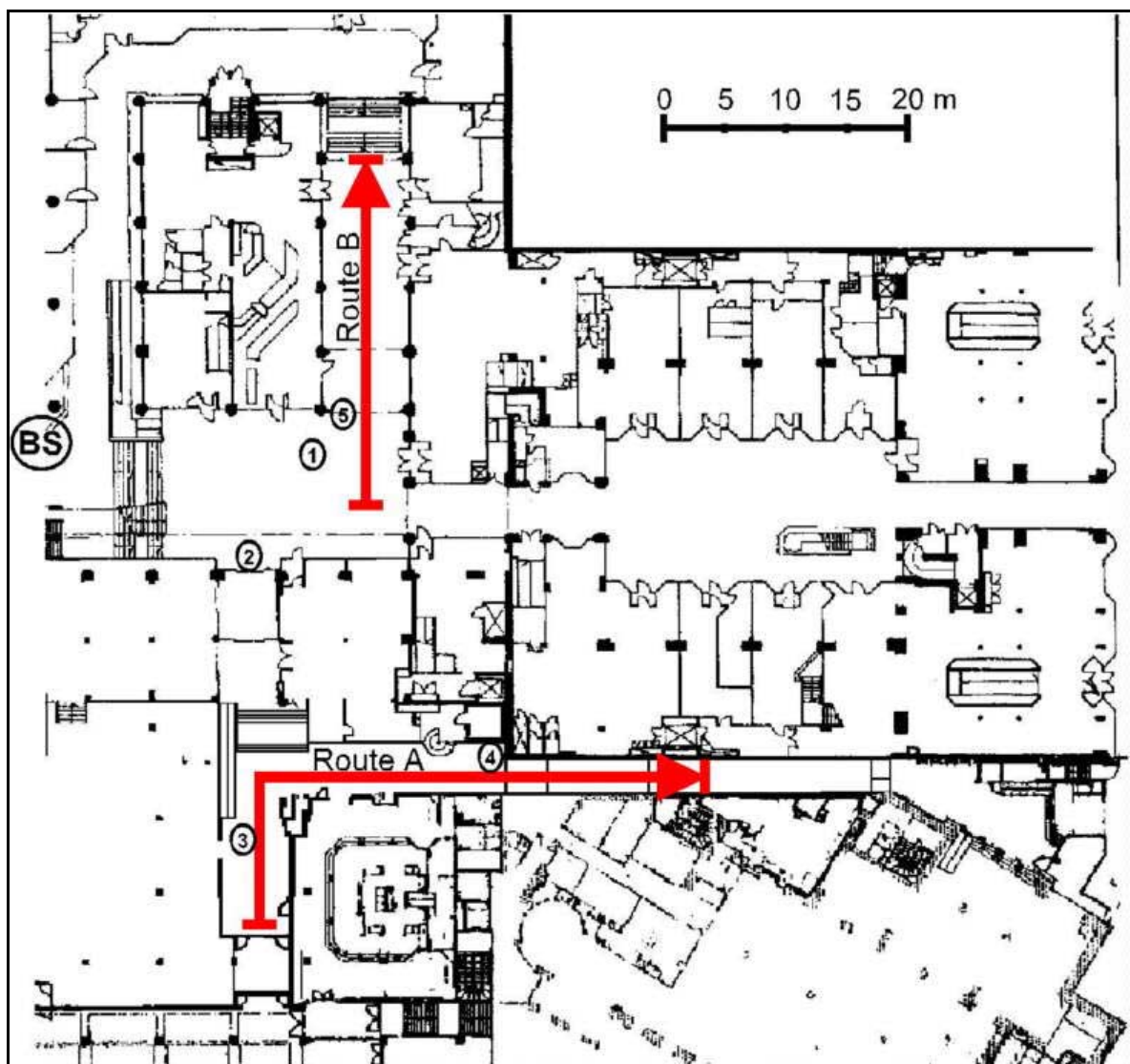


Figure 2. Floor plan of the measurement site.

Table 1. Mobile routes.

	Length	Number of IRs	Type
Route A	50 m	1800 IRs	indoor
Route B	30 m	1100 IRs	outdoor

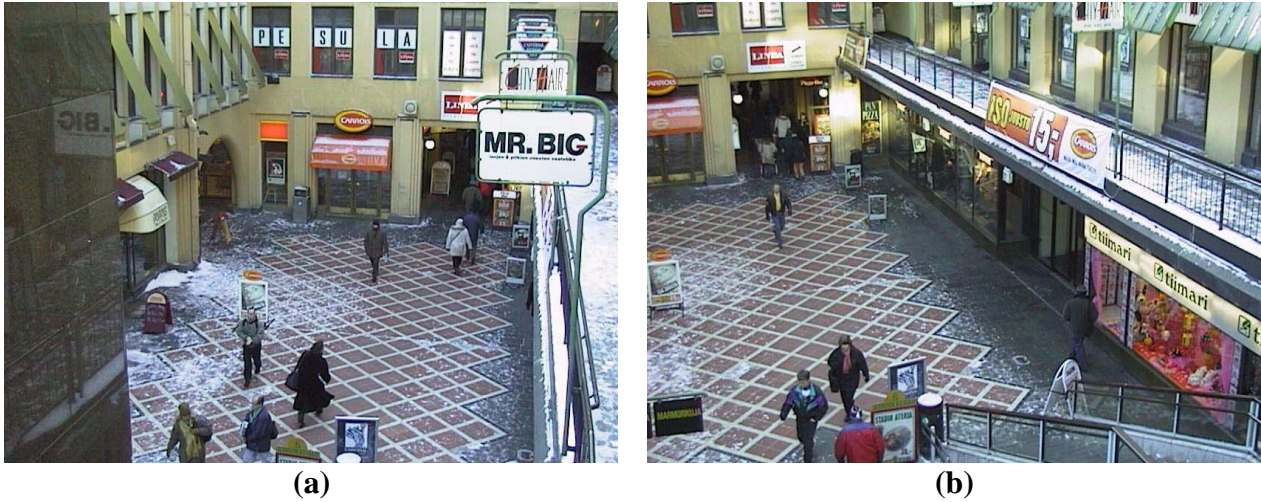


Figure 3. View from the BS location towards the mobile routes. The doorway leading to the indoor route (marked as ② in Fig. 2). can be seen at right in (b). The underpass ⑤ can be seen at left in (a).



Figure 4. View from point ① towards the BS location. The position of the BS antenna in the measurements has been marked in the picture.

5. Analysis of measurement data

The goal of the data analysis was to discover dynamically evolving propagation paths from the complex impulse responses gathered over a specified measurement route. This was achieved in two

phases. In the first phase a discrete number of impinging waves was found at each receiver location by going through the following steps:

- 1) Compute the power delay profile (PDP) and search for local maxima exceeding a threshold power level
- 2) For each PDP peak, compute the direction-of-arrival (DOA) power spectrum by beamforming and search for local maxima exceeding a threshold power level
- 3) Store the DOA, delay, amplitude, and phase for both VP and HP components

In step 1) the PDP was calculated by considering only the element that receives the maximum power at each delay sample. This way the dynamics of the PDP measurement is maximized. In step 2) a grid of beams was formed with 2° resolution in the azimuth and elevation angles [5]. A threshold of 6 dB below the maximum was used to suppress the sidelobes. Finally, in step 3), at most 4 local DOA maxima at each PDP peak were stored.

At the second phase, the waves impinging at the receiver at successive locations were combined to form continuous paths. Two waves at successive receiver locations were joined if the delays and the DOAs differed at most by one delay sample and 15° , respectively. Moreover, a path was stored only if it existed for five consecutive receiver locations (one wavelength). As a result, spurious signals were efficiently filtered and the obtained path data contains the dominant propagation paths.

6. Measurement results

Power Azimuth Spectrum

The measured indoor and outdoor power azimuth spectra (PAS) averaged over the mobile routes are presented in Figure 5. The effect of distance-dependent path loss to the received power has been removed, and the result has been normalized to the maximum. Zero azimuth angle corresponds to the mobile moving direction.

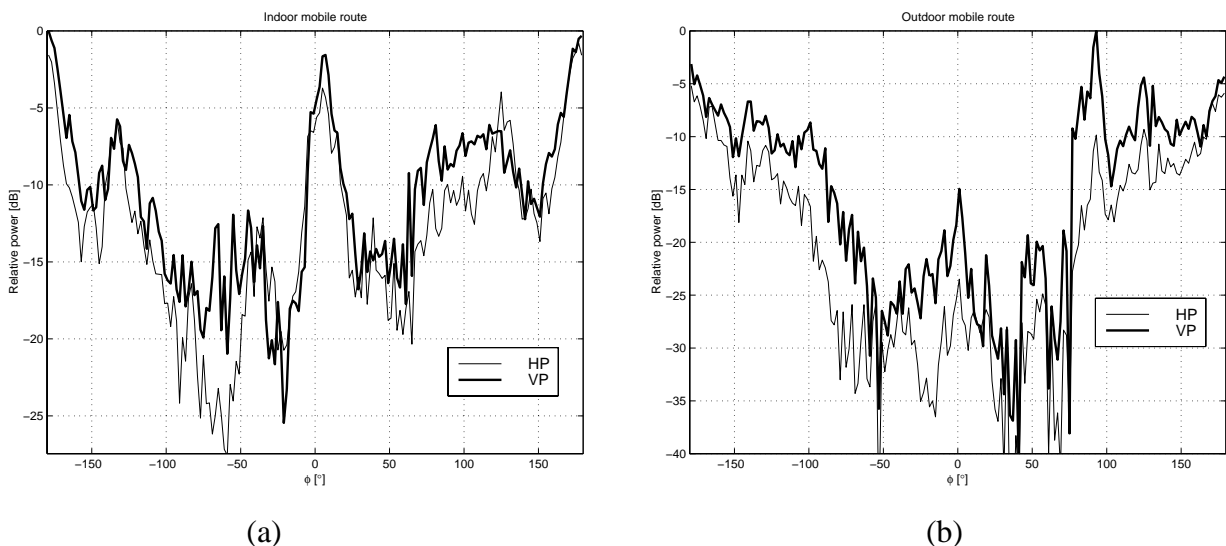


Figure 5. Measured average power azimuth spectra of the incident waves. (a) indoor. (b) outdoor.

It can be seen that the propagation along the corridor dominates at the indoor mobile route, Figure 5 (a). Peaks can be seen at the directions corresponding to the mobile moving direction and the opposite direction. In the outdoor case, the LOS peak can be seen approximately at $+90^\circ$ (left), and most of the power is received from behind when looking at the mobile moving direction, which is expected since the mobile is moving away from the BS. There seems to be no significant difference between the distributions of the two polarizations, except that the LOS peak is much more pronounced in the VP spectrum. The PAS measured in the indoor route is more uniform which can be explained by the longer and more versatile route.

Power Elevation Spectrum

The measured indoor and outdoor power elevation spectra (PES) averaged over the mobile routes are presented in Figure 6. The effect of distance-dependent path loss to the received power has been removed, and the result has been normalized to the maximum. The elevation angle is measured from the horizontal plane.

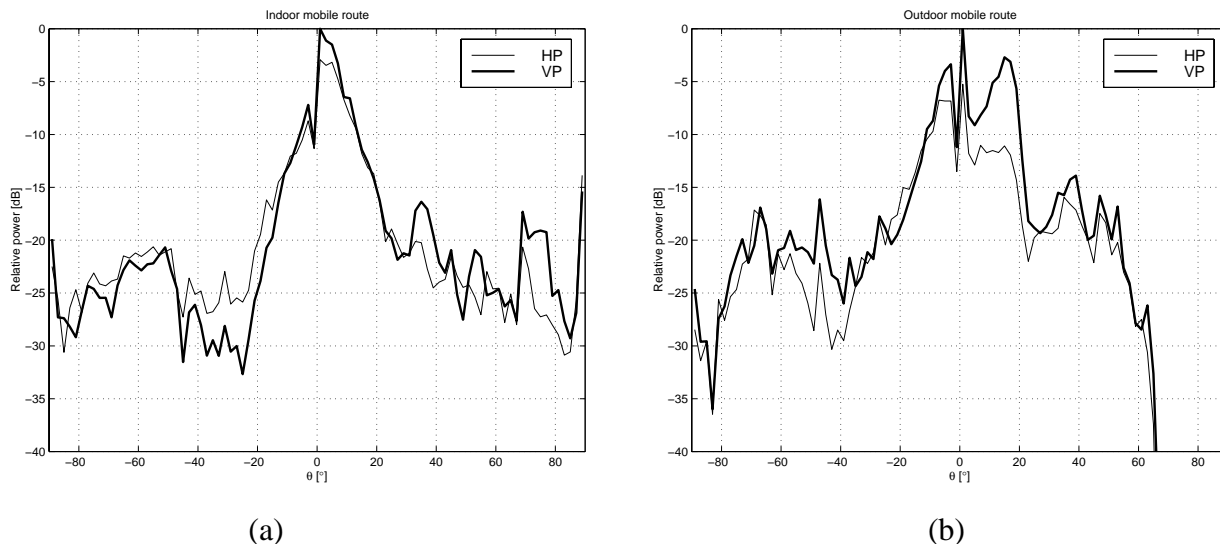


Figure 6. Measured average power elevation spectra of the incident waves. (a) indoor. (b) outdoor.

In the indoor case most of the power is concentrated slightly above the horizontal plane. The distributions of HP and VP components seem to be quite similar, except of the region between -40° and -20° , where the horizontal polarization dominates. The spectrum resembles a Gaussian distribution around the horizontal plane, where most of the power is concentrated. Elsewhere the distribution seems quite uniform, except of the clear minimum in the incident power at VP at $-40^\circ \dots 20^\circ$. In the outdoor route no power is received above $+65^\circ$, which is quite reasonable. Instead, the effect of ground reflections can clearly be seen. In both spectra, the strongest peak is at the horizontal plane. Also the outdoor spectrum resembles gaussian, and the three peaks are assumed to be due to the limited environment. In the VP spectrum, the LOS peak at 15° is emphasized. The mean and standard deviation of the measured elevation angle are presented in Table 2. Unfortunately, comparison with Taga's results [1] is not possible due to different environment type.

Table 2. Mean and standard deviation of elevation angle.

	VP	HP
Indoor	$m_V = 5.1^\circ, \sigma_V = 17.6^\circ$	$m_H = 3.9^\circ, \sigma_H = 20.0^\circ$
Outdoor	$m_V = 4.3^\circ, \sigma_V = 17.5^\circ$	$m_H = -1.0^\circ, \sigma_H = 21.6^\circ$

Doppler Spectrum

The measured indoor and outdoor Doppler spectra averaged over the mobile routes are presented in Figure 7. The effect of distance-dependent path loss to the received power has been removed, and the result has been normalized to the maximum.

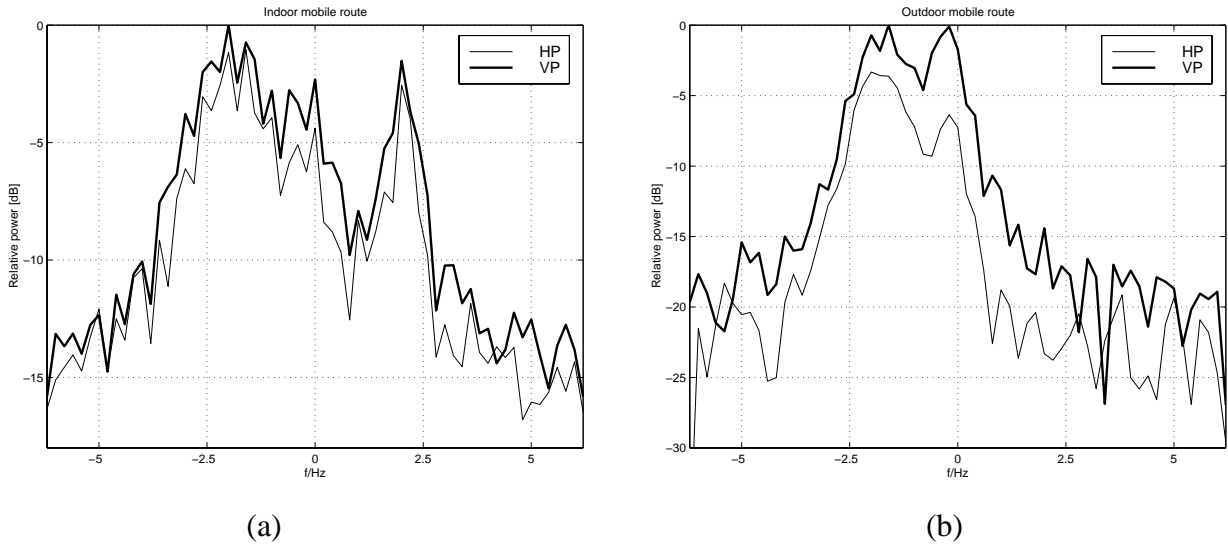


Figure 7. Measured average Doppler spectra of the incident waves. (a) indoor. (b) outdoor.

A comparison of the Doppler spectra and the azimuth spectra shows good consistency. In the indoor case, the peaks in the PAS correspond to Doppler shifts of ± 2.5 Hz, assuming that the elevation DOA is 0° . The peaks of the Doppler spectrum are found at slightly lower Doppler shifts which is reasonable since all waves do not travel in the horizontal plane. Similarly, in the outdoor case, the waves arriving from behind the receiver are shown as a peak at negative Doppler frequencies. The LOS peak at approximately 0 Hz is pronounced in the VP spectrum as expected. As in the azimuth spectrums, the indoor case shows more uniform behavior. The mean and standard deviation of the measured Doppler frequency are presented in Table 3.

Table 3. Mean and standard deviation of Doppler frequency.

	VP	HP
Indoor	$m_V = -0.67 \text{ Hz}, \sigma_V = 2.3 \text{ Hz}$	$m_H = -0.75 \text{ Hz}, \sigma_H = 2.27 \text{ Hz}$
Outdoor	$m_V = -1.0 \text{ Hz}, \sigma_V = 1.4 \text{ Hz}$	$m_H = -1.4 \text{ Hz}, \sigma_H = 1.4 \text{ Hz}$

7. Conclusions

This paper presents measured statistical distributions of incident waves to a mobile antenna in microcellular environment at 2.15 GHz. The power spectra of azimuth angle, elevation angle, and Doppler frequency are presented separately for horizontally and vertically polarized waves. The measurements were made along one outdoor and one indoor route. The collected data corresponds to a restricted environment, thus no profound conclusions can be made. However, Taga's [1] assumption of Gaussian distribution of the elevation angle seems to be valid. Extensive measurement campaigns are required to define the overall distribution parameters.

The measurement results show that the used measurement technique is an efficient tool for characterizing mobile propagation environments. The measured elevation angle distributions are reasonable, and the measured power azimuth spectrum agrees with the Doppler spectrum. Complete angular and polarization statistics of the incident waves at the mobile can be found through extensive measurement campaigns. The statistics can be used for evaluating the mean effective gain of mobile antennas.

References

- [1] T. Taga, "Analysis for Mean Effective Gain of Mobile Antennas in Land Mobile Radio Environments," *IEEE Transactions on Vehicular Technology*, Vol. VT-39, No. 2, May 1990, pp. 117-131.
- [2] T. Aulin, "A Modified Model for the Fading Signal at a Mobile Radio Channel" *IEEE Transactions on Vehicular Technology*, Vol. VT-28, No. 3, 1979, pp. 182-203.
- [3] D. Parsons, *The Mobile Propagation Channel*, London, Pentech Press, 1992, 316 p.
- [4] R.G. Vaughan, "Antenna Diversity in Mobile Communications" *IEEE Transactions on Vehicular Technology*, Vol. VT-36, No. 4, Nov. 1987, pp. 149-172.
- [5] K. Kalliola, "Directional 3D Real-time Dual-polarized Measurement of Wideband Mobile Radio Channel", *COST 259 Temporary Document TD(98)13*, Thessaloniki, Greece, January 20-22, 1999.